This article has been accepted for publication in IEEE Control Systems Letters. This is the author's version which has not been fully edited and content may change prior to final publication. Citation information: DOI 10.1109/LCSYS.2023.3331245

Formation Control on Planar Closed Curves Using Fourier Descriptors

Miguel Aranda, *Member, IEEE*

***Abstract*— This article proposes a novel way of specifying and controlling planar multiagent formations, based on Fourier descriptors. We consider a given ordering of the agents in a sequence, and address the problem of controlling the discretized curve formed by the sequence of agent positions. In particular, we propose to make the agents form a specific type of curve: one that can be parameterized with a selected number of low-frequency Fourier descriptors. To achieve this, we present a gradient-descent control approach that exploits the structure of the discrete Fourier transform (DFT). We propose control laws for single-integrator and double-integrator agent models and show formally the convergence to a closed curve of the targeted type. We also study several relevant features of the resulting system: dynamics of the team's scale and centroid, robustness to perturbation, and implementation in local frames. With our approach the agents form a low-frequency discretized closed curve with an adaptable shape not tied to a prescribed geometric pattern. This can be useful, e.g., in target enclosing tasks. We present illustrative simulation examples.**

***Index Terms*— Cooperative control, autonomous systems, robotics.**

I. Introduction

THE problem of controlling a formation [1] is relevant for various multiagent tasks including area monitoring, navigation, object transport, and target enclosing. In such tasks, it is useful to prescribe a favorable geometric arrangement (i.e., a desired formation) and then control the agents so that they stay close to this arrangement during execution. Different approaches have been proposed for encoding the desired formation. A popular option is to encode it at the agent level, in terms of absolute or relative positions, distances, or angular information [2]–[5]; then, in the desired formation the agents form a pattern equal to a prescribed one up to a specific type of transformation (e.g., rigid or affine).

An alternative option is to encode the desired formation as a whole in an abstract manner. One advantage of this is that the resulting representation is lower-dimensional. For example, the abstract state in [6] consists of a position, an orientation, and a concentration ellipse that characterizes the distribution of agents. Similarly, geometric moment statistics are exploited for encoding a desired formation in [7]. The study [8] presents a control law for a swarm of agents such that the swarm aggregates in a polytope around a desired position in space in finite time. In [9], a continuification-based approach is proposed to distribute a team of agents moving along a ring according to a desired density profile.

Here, we propose to use Fourier descriptors [10], [11], i.e., coefficients of the discrete Fourier transform (DFT), to represent a desired formation on a planar closed curve. One popular use of this formalism is for encoding a curve in a compact way using a reduced number of low-frequency descriptors [12]. This is exploited for representing the contour of a deformable object during a robotic manipulation task in [13]. In the domain of multiagent control, an approach proposed in [14] uses Fourier descriptors to make the agents first reach positions in a closed curve (an ellipse) and then move toward another prescribed closed curve. In the study [15], a multiagent formation control approach is used to track a closed boundary in the environment. The authors achieve a suitable distribution of the agents by representing the boundary as a parametric curve using Fourier descriptors.

Our approach considers a team of agents ordered in a given sequence. Then, we define the desired formation as any team configuration where the ordered sequence of agent positions forms a discretized closed curve that can be represented with a selected set of low-frequency Fourier descriptors. Compared to [14], [15], the problem we address is different, as we do not consider an externally prescribed boundary (i.e., closed curve) to be reached by the multiagent team. In more detail, we (i) truncate the set of descriptors of the curve formed by the agents at any given instant and (ii) move the agents toward the curve represented by that truncated set of descriptors. Exploiting the properties of the DFT, we formulate this as a gradient-descent approach, proposing control laws for single-integrator and double-integrator dynamics. These control laws use the current positions/velocities of all agents. We analyze the convergence of the control laws, the evolutions of the centroid and scale of the team, and the robustness to perturbation. We also discuss implementation requirements, and present illustrative simulation examples.

Our novel approach allows agents to distribute themselves along a discretized planar closed curve having only low-frequency content (i.e., an ellipse or a more complex curve). With the proposed frequency-domain formation specification, the team's shape in the general case is not associated with a specific prescribed geometric pattern; in this respect, our ap-

This work was supported by MCIN/AEI/10.13039/501100011033, the ERDF A way of making Europe, and the European Union NextGenerationEU/PRTR under Projects PID2021-124137OB-I00 and TED2021-130224B-I00; and by the Spanish Ministry of Universities and the European Union-NextGenerationEU under a María Zambrano Fellowship.

The author is with the Instituto de Investigación en Ingeniería de Aragón (I3A), Universidad de Zaragoza, 50018 Zaragoza, Spain (e-mail: miguel.aranda@unizar.es).

This article has been accepted for publication in IEEE Control Systems Letters. This is the author's version which has not been fully edited and content may change prior to final publication. Citation information: DOI 10.1109/LCSYS.2023.3331245

proach differs from existing works [2]–[5], [16], [17]. Unlike the approaches in [2]–[5], our approach is not able to achieve any arbitrary prescribed pattern, as it only achieves low-frequency curves. However, its key advantage is it achieves closed curves without sharp variations and whose shape is more adaptable than with [2]–[5], [16], [17]; these features are interesting, e.g., for target enclosing tasks [16], [17].

A. Notation

The symbols $\otimes$, $||\cdot||$, $\mathbf{I}_N$ and $\mathbf{1}_N$ denote, respectively, the Kronecker product, the Euclidean norm, the $N \times N$ identity matrix, and a column vector of N ones. We denote $j = \sqrt{-1}$. For compactness, we sometimes do not write the time dependence (t). We use $(\cdot)$ to denote ordered sequences, and $\{\cdot\}$ to denote unordered sets. We express angles in radians.

II. Problem formulation

We consider a team of N mobile agents ($N > 3$) in the plane, and assign each of them a different index in the set $\mathcal{N} = \{0, 1, ..., N-1\}$. The position of every agent is denoted by a column vector $\mathbf{p}_n \in \mathbb{R}^2$ for every $n \in \mathcal{N}$. These positions are expressed in an arbitrary fixed reference frame. We use $\mathbf{p} = [\mathbf{p}_0^\intercal, ..., \mathbf{p}_{N-1}^\intercal]^\intercal \in \mathbb{R}^{2N}$ as a stack vector containing the agent positions. We consider two different dynamic models for the agents: (i) single-integrator, where $\dot{\mathbf{p}} = \mathbf{u}$, and (ii) double-integrator, where $\dot{\mathbf{p}} = \mathbf{v}$, $\dot{\mathbf{v}} = \mathbf{u}$. In both cases, $\mathbf{u} = [\mathbf{u}_0^\intercal, ..., \mathbf{u}_{N-1}^\intercal]^\intercal \in \mathbb{R}^{2N}$ represents the control input for the team, and $\mathbf{u}_n \in \mathbb{R}^2$ represents the control input for agent n.

A. Background: DFT and Fourier descriptors

The DFT is a widely used tool described in many sources, e.g., in [10, Ch. 5], [11, Ch. 4]. Given a sequence of N complex numbers $(p_0, ..., p_{N-1})$, its DFT is a sequence of N complex numbers $(d_0, ..., d_{N-1})$ computed as

$$d_k = \sum_{n=0}^{N-1} p_n e^{-j2\pi kn/N}, \quad k = 0, 1, ..., N-1. \tag{1}$$

The DFT represents uniquely the sequence $(p_0, ..., p_{N-1})$ in the frequency domain. In turn, we can recover the sequence from its DFT using the inverse DFT (IDFT), defined as

$$p_n = \frac{1}{N} \sum_{k=0}^{N-1} d_k e^{j2\pi kn/N}, \quad n = 0, 1, ..., N-1. \tag{2}$$

One application of the DFT is the representation of planar curves defined as sequences of points [11, Ch. 11], [12]–[15]. For this purpose, the real and imaginary parts of p_n are interpreted as the $x-y$ position coordinates of a point n in the plane. In our case, the points are the agents' positions, and thus the 1D representation $p_n = x_n + jy_n$ becomes the 2D representation $\mathbf{p}_n = [x_n, y_n]^\intercal \in \mathbb{R}^2$ introduced above.

Let us define the ordered sequence of 2D agent positions $\mathtt{P} = (\mathbf{p}_0, ..., \mathbf{p}_{N-1})$. To formulate the DFT in terms of this representation, we first define the rotation matrix

$$\mathbf{R}_l = \begin{bmatrix} \cos(-2\pi l/N) & -\sin(-2\pi l/N) \\ \sin(-2\pi l/N) & \cos(-2\pi l/N) \end{bmatrix}, \tag{3}$$

where l is a natural number. Note that $\mathbf{R}_0 = \mathbf{I}_2$. Then, we define the DFT of $\mathtt{P}$ as a sequence $\mathtt{D} = (\mathbf{d}_0, ..., \mathbf{d}_{N-1})$ with

$$\mathbf{d}_k = \sum_{n=0}^{N-1} \mathbf{R}_{kn} \mathbf{p}_n, \quad k = 0, 1, ..., N-1. \tag{4}$$

We call the N elements of $\mathtt{D}$ the Fourier descriptors of $\mathtt{P}$ [11, Ch. 11]. Note that each $\mathbf{d}_k \in \mathbb{R}^2$ is equivalent to the d_k of (1). Similarly, for the IDFT we have

$$\mathbf{p}_n = \frac{1}{N} \sum_{k=0}^{N-1} \mathbf{R}_{kn}^\intercal \mathbf{d}_k, \quad n = 0, 1, ..., N-1. \tag{5}$$

An interesting fact is that, treating the sequences $\mathtt{P}$ and $\mathtt{D}$ as stack vectors, the DFT can be expressed as a linear transformation [10, Ch. 5]. For this, we define stack vectors $\mathbf{p} = [\mathbf{p}_0^\intercal, ..., \mathbf{p}_{N-1}^\intercal]^\intercal \in \mathbb{R}^{2N}$ and $\mathbf{d} = [\mathbf{d}_0^\intercal, ..., \mathbf{d}_{N-1}^\intercal]^\intercal \in \mathbb{R}^{2N}$. Note that $\mathbf{p}$ is our definition for the state of the team given earlier on in Sec. II. Based on (4), (5), we can define the following transformation matrices of size $2N \times 2N$:

$$\mathbf{M} = \begin{bmatrix} \mathbf{I}_2 & \mathbf{I}_2 & \mathbf{I}_2 & ... & \mathbf{I}_2 \\ \mathbf{I}_2 & \mathbf{R}_1 & \mathbf{R}_2 & ... & \mathbf{R}_{N-1} \\ \mathbf{I}_2 & \mathbf{R}_2 & \mathbf{R}_4 & ... & \mathbf{R}_{2(N-1)} \\ ... & ... & ... & ... & ... \\ \mathbf{I}_2 & \mathbf{R}_{N-1} & \mathbf{R}_{2(N-1)} & ... & \mathbf{R}_{(N-1)(N-1)} \end{bmatrix}, \tag{6}$$

$$\mathbf{M}_I = \frac{1}{N} \begin{bmatrix} \mathbf{I}_2 & \mathbf{I}_2 & \mathbf{I}_2 & ... & \mathbf{I}_2 \\ \mathbf{I}_2 & \mathbf{R}_1^\intercal & \mathbf{R}_2^\intercal & ... & \mathbf{R}_{N-1}^\intercal \\ \mathbf{I}_2 & \mathbf{R}_2^\intercal & \mathbf{R}_4^\intercal & ... & \mathbf{R}_{2(N-1)}^\intercal \\ ... & ... & ... & ... & ... \\ \mathbf{I}_2 & \mathbf{R}_{N-1}^\intercal & \mathbf{R}_{2(N-1)}^\intercal & ... & \mathbf{R}_{(N-1)(N-1)}^\intercal \end{bmatrix}. \tag{7}$$

Observe that $\mathbf{d} = \mathbf{M}\mathbf{p}$ for the DFT, and $\mathbf{p} = \mathbf{M}_I \mathbf{d}$ for the IDFT. This implies $\mathbf{M}_I$ is the inverse of $\mathbf{M}$, i.e., $\mathbf{M}^{-1} = \mathbf{M}_I$. Also, from the form of the matrices one sees that $\mathbf{M}_I = \mathbf{M}^{-1} = (1/N)\mathbf{M}^\intercal$. Note that $\mathbf{M}$, $\mathbf{M}_I$ are constant matrices and they are fully determined by the number of agents, N.

B. Selection of Fourier descriptors

Fourier descriptors are often used for representing planar closed curves compactly. One selects a reduced number of low-frequency descriptors of the original curve and disregards the rest [11, Ch. 11], [12]–[15]. This results in a curve that approximates the original one, eliminating fine detail and sharp variation (associated with high frequencies) while retaining the global curve shape, encoded in the low-frequency descriptors. In this article, we use a similar technique. The first step of our design is choosing the number H of descriptors to use, with $1 < H < N$. For convenience, we take H as an odd number. Then, we define $\mathcal{H}$, the selected set of indices of the descriptors corresponding to H, as

$$\mathcal{H} = \{0, 1, ..., (H-1)/2, N-(H-1)/2, ..., N-1\}. \tag{8}$$

These indices are the low frequencies up to index $(H-1)/2$. $\mathcal{H}$ includes both the positive and the negative frequencies around the zero frequency, and its definition takes into account that frequencies loop circularly in the DFT: e.g., note in (1) or

This article has been accepted for publication in IEEE Control Systems Letters. This is the author's version which has not been fully edited and content may change prior to final publication. Citation information: DOI 10.1109/LCSYS.2023.3331245

(4) that the term for $k = N$ would be equal to the term for $k = 0$. The way we use the selected descriptors is different from prior uses for curve representation applications. Here, our idea is to move the agents toward a configuration whose Fourier descriptors are zero for indices outside of the selected set $\mathcal{H}$. The details are given next.

C. Desired formation and problem statement

We define the core element of the addressed problem next.

Definition 1 (Desired formation): We say that the team of agents in a configuration $\mathbf{p}$ is in the desired formation if the Fourier descriptors of $\mathtt{P}$, i.e., the components $\mathbf{d}_k$ of $\mathtt{D}$, are zero $\forall k \in \mathcal{N} - \mathcal{H}$.

Note that the desired formation is not a unique configuration; there is clearly an infinite set of configurations $\mathbf{p}$ that satisfy Def. 1. The definition is in terms of the frequency properties of the sequence of positions $\mathtt{P}$, and it means that this sequence only has low-frequency content. Next, we describe the desired formation more concretely, using Fourier-based parametric curve representation concepts [11, Ch. 11], [15].

Let us suppose that the team is in the desired formation. We can see by direct manipulations of the IDFT (5) that

$$\mathbf{p}_n = \mathbf{v}_0 + \sum_{k=1}^{(H-1)/2} \mathbf{c}_k \cos\Big(\frac{2\pi k n}{N}\Big) + \mathbf{s}_k \sin\Big(\frac{2\pi k n}{N}\Big), \text{ with } (9)$$

$$\mathbf{v}_0 = \frac{1}{N}\mathbf{d}_0,\ \mathbf{c}_k = \frac{1}{N}(\mathbf{d}_k + \mathbf{d}_{N-k}),\ \mathbf{s}_k = \frac{1}{N}\mathbf{T}(\mathbf{d}_k - \mathbf{d}_{N-k}),$$

for $n = 0, ..., N-1$ and $\mathbf{T}$ defined as $\mathbf{T} = [[0,1]^\intercal, [-1,0]^\intercal]$. Terms can be grouped in the single sum of (9) due to symmetry of the sinusoids. Let us now consider the parametric curve $\mathbf{p}^s : s \to \mathbb{R}^2$, where $s \in [0, N) \in \mathbb{R}$ is a continuously defined parameter, with the following expression:

$$\mathbf{p}^s = \mathbf{v}_0 + \sum_{k=1}^{(H-1)/2} \mathbf{c}_k \cos\Big(\frac{2\pi k s}{N}\Big) + \mathbf{s}_k \sin\Big(\frac{2\pi k s}{N}\Big). \quad (10)$$

Note that $\mathbf{p}^s$ is a closed curve, due to the periodicity of the sinusoidal terms. It is direct to see that (9) is a discretized, sampled version of (10); concretely, $\mathbf{p}_n = \mathbf{p}^s\rfloor_{s=n}$. Therefore, any configuration where the team is in the desired formation is a discretized closed curve created by a sum of sinusoids. Let us illustrate the particular case $H = 3$; i.e., we take $\mathcal{H} = \{0, 1, N-1\}$. This means that only three of the Fourier descriptors are selected. Then, from (9),

$$\mathbf{p}_n = \mathbf{v}_0 + \mathbf{c}_1 \cos\Big(\frac{2\pi n}{N}\Big) + \mathbf{s}_1 \sin\Big(\frac{2\pi n}{N}\Big), \quad (11)$$

with $n = 0, ..., N-1$, and from (10):

$$\mathbf{p}^s = \mathbf{v}_0 + \mathbf{c}_1 \cos\Big(\frac{2\pi s}{N}\Big) + \mathbf{s}_1 \sin\Big(\frac{2\pi s}{N}\Big). \quad (12)$$

Note that (12) is the standard parametric representation of an ellipse. Therefore, when the team is in the desired formation the sequence of agent positions forms a discretized ellipse. Hence, for this particular case, the team forms a specific (i.e., elliptical) pattern. In the general case, with higher H, more complex curves (i.e., with more sinusoidal terms) than an ellipse are obtained and the team does not form a prescribed geometric pattern. Such more complex curves provide higher formation flexibility. Since $H < N$, with more agents the complexity of the curves that can be achieved also grows.

Considering the above, the problem we address is designing a control strategy to drive the team to the desired formation.

III. Proposed formation control approach

Next, we present our solution to the stated problem. We define the truncated DFT of $\mathtt{P}$ according to the set $\mathcal{H}$ as the sequence $\mathtt{D}^{\mathcal{H}} = (\mathbf{d}_0^{\mathcal{H}}, ..., \mathbf{d}_{N-1}^{\mathcal{H}})$ with

$$\mathbf{d}_k^{\mathcal{H}} = \begin{cases} \sum_{n=0}^{N-1} \mathbf{R}_{kn}\mathbf{p}_n, & k \in \mathcal{H} \\ \mathbf{0}, & k \in \mathcal{N} - \mathcal{H} \end{cases}. \quad (13)$$

We also define the vector stacking the components of $\mathtt{D}^{\mathcal{H}}$ as $\mathbf{d}^{\mathcal{H}} = [(\mathbf{d}_0^{\mathcal{H}})^\intercal, ..., (\mathbf{d}_{N-1}^{\mathcal{H}})^\intercal]^\intercal$. The IDFT of $\mathtt{D}^{\mathcal{H}}$, called $\mathtt{P}^{\mathcal{H}} = (\mathbf{p}_0^{\mathcal{H}}, ..., \mathbf{p}_{N-1}^{\mathcal{H}})$, is as follows:

$$\mathbf{p}_n^{\mathcal{H}} = \frac{1}{N}\sum_{k=0}^{N-1} \mathbf{R}_{kn}^\intercal \mathbf{d}_k^{\mathcal{H}}, \quad n = 0, 1, ..., N-1. \quad (14)$$

Let us define $\mathbf{p}^{\mathcal{H}} = [(\mathbf{p}_0^{\mathcal{H}})^\intercal, ..., (\mathbf{p}_{N-1}^{\mathcal{H}})^\intercal]^\intercal$. Note, from Def. 1, that if $\mathbf{p} = \mathbf{p}^{\mathcal{H}}$, the team is in the desired formation. Next, we formulate the described truncation operation via a diagonal selection matrix. For this we define $\mathbf{Q}_{\mathcal{H}} \in \mathbb{R}^{N\times N}$ for $i = 1, ..., N$, $l = 1, ..., N$ as

$$\mathbf{Q}_{\mathcal{H}}[i,l] = \begin{cases} 1, & i = l \text{ and } (i-1) \in \mathcal{H} \\ 0, & \text{otherwise} \end{cases}. \quad (15)$$

Then, we define our selection matrix as $\mathbf{S}_{\mathcal{H}} = \mathbf{Q}_{\mathcal{H}} \otimes \mathbf{I}_2$. Note that $\mathbf{S}_{\mathcal{H}}^\intercal = \mathbf{S}_{\mathcal{H}}$ and $\mathbf{S}_{\mathcal{H}}^2 = \mathbf{S}_{\mathcal{H}}$. Observe that we have $\mathbf{d}^{\mathcal{H}} = \mathbf{S}_{\mathcal{H}}\mathbf{d} = \mathbf{S}_{\mathcal{H}}\mathbf{M}\mathbf{p}$. Conversely, we also have $\mathbf{p}^{\mathcal{H}} = (1/N)\mathbf{M}^\intercal\mathbf{d}^{\mathcal{H}}$. Putting things together we get

$$\mathbf{p}^{\mathcal{H}}(t) = \mathbf{A}\mathbf{p}(t), \quad \text{with } \mathbf{A} = \frac{1}{N}\mathbf{M}^\intercal\mathbf{S}_{\mathcal{H}}\mathbf{M}. \quad (16)$$

This way, we have represented $\mathbf{p}^{\mathcal{H}}(t)$ as a linear transformation of $\mathbf{p}(t)$, encoded by the constant matrix $\mathbf{A}$. Two useful properties of $\mathbf{A}$ are that it is symmetric and idempotent. To see the latter, first notice that $\mathbf{A}^2 = (1/N^2)\mathbf{M}^\intercal\mathbf{S}_{\mathcal{H}}\mathbf{M}\mathbf{M}^\intercal\mathbf{S}_{\mathcal{H}}\mathbf{M}$. Recalling from Sec. II-A that $\mathbf{M}^\intercal = N\mathbf{M}^{-1}$, we have $\mathbf{M}\mathbf{M}^\intercal = N\mathbf{I}_{2N}$. By substitution of this identity and of $\mathbf{S}_{\mathcal{H}}^2 = \mathbf{S}_{\mathcal{H}}$, we directly find $\mathbf{A}^2 = \mathbf{A}$.

We can obtain a more explicit expression of $\mathbf{A}$ via algebraic manipulation and by exploiting symmetry properties of sinusoids: concretely, $\mathbf{A} = \mathbf{B} \otimes \mathbf{I}_2$ where $\mathbf{B} \in \mathbb{R}^{N\times N}$ has the following entries for $i = 1, ..., N$, $l = 1, ..., N$:

$$\mathbf{B}[i,l] = \frac{1}{N}\Big(1 + 2\sum_{k=1}^{(H-1)/2} \cos\Big(\frac{2\pi(l-i)k}{N}\Big)\Big). \quad (17)$$

$\mathbf{p}^{\mathcal{H}}(t)$ can be thought of as the result of projecting $\mathbf{p}(t)$ onto the space of all configurations where the team is in the desired formation. Our idea is to treat $\mathbf{p}^{\mathcal{H}}(t)$ as a destination configuration. We thus propose a control strategy, described next, to move the team so that $\mathbf{p}(t)$ approaches $\mathbf{p}^{\mathcal{H}}(t)$.

This article has been accepted for publication in IEEE Control Systems Letters. This is the author's version which has not been fully edited and content may change prior to final publication. Citation information: DOI 10.1109/LCSYS.2023.3331245

A. Control strategy

We propose a gradient-based control strategy to make the team move toward $\mathbf{p}^{\mathcal{H}}(t)$. Consider the cost

$$\gamma(t) = \frac{1}{2}||\mathbf{p}^{\mathcal{H}}(t) - \mathbf{p}(t)||^2. \tag{18}$$

From (16), and as $\mathbf{A}$ is symmetric and idempotent, we get

$$\gamma(t) = (1/2)\mathbf{p}^{\intercal}(t)(\mathbf{I}_{2N} - \mathbf{A})\mathbf{p}(t). \tag{19}$$

Notice that $\mathbf{I}_{2N} - \mathbf{A}$ is positive semidefinite, because $\gamma(t) \geq 0$ (18). Since $\mathbf{A}$ is symmetric, the negative gradient of γ with respect to the positions $\mathbf{p}$ is

$$-\nabla_{\mathbf{p}}\gamma(t) = \mathbf{p}^{\mathcal{H}}(t) - \mathbf{p}(t) = (\mathbf{A} - \mathbf{I}_{2N})\mathbf{p}(t). \tag{20}$$

The main idea of our control strategy is to move the agents at every instant t in the direction of this negative gradient, so as to make $\gamma(t) = 0$ and thus $\mathbf{p}(t) = \mathbf{p}^{\mathcal{H}}(t)$. For single-integrator dynamics, we propose the control law

$$\mathbf{u}(t) = \kappa(\mathbf{p}^{\mathcal{H}}(t) - \mathbf{p}(t)) = \kappa(\mathbf{A} - \mathbf{I}_{2N})\mathbf{p}(t), \tag{21}$$

where $\kappa > 0$ is a real scalar. This control law directly follows the direction of the negative gradient. For double-integrator dynamics, we propose the control law

$$\begin{aligned}\mathbf{u}(t) &= \kappa_1(\mathbf{p}^{\mathcal{H}}(t) - \mathbf{p}(t)) + \kappa_2(\dot{\mathbf{p}}^{\mathcal{H}}(t) - \dot{\mathbf{p}}(t)) \\ &= \kappa_1(\mathbf{A} - \mathbf{I}_{2N})\mathbf{p}(t) + \kappa_2(\mathbf{A} - \mathbf{I}_{2N})\dot{\mathbf{p}}(t),\end{aligned} \tag{22}$$

where $\kappa_1 > 0$, $\kappa_2 > 0$ are real scalars. This control law is also based on following the negative gradient direction, while taking into account the second-order dynamics.

B. Stability analysis

We study the proposed control strategy next. For this study, we define the control error $\mathbf{e} = [\mathbf{e}_0^{\intercal}, ..., \mathbf{e}_{N-1}^{\intercal}]^{\intercal} \in \mathbb{R}^{2N}$ as

$$\mathbf{e}(t) = \mathbf{p}(t) - \mathbf{p}^{\mathcal{H}}(t), \tag{23}$$

i.e., $\gamma(t) = (1/2)||\mathbf{e}(t)||^2$. We first consider the control (21).

Theorem 1: Under the single-integrator control law (21), $\mathbf{p}^{\mathcal{H}}(t)$ is invariant and the control error $\mathbf{e}(t)$ converges to zero globally and exponentially fast.

Proof: For single-integrator dynamics, $\dot{\mathbf{p}}(t) = \mathbf{u}(t)$. The invariance of $\mathbf{p}^{\mathcal{H}}(t)$ follows by considering its dynamics under (21) and using $\mathbf{A}^2 = \mathbf{A}$, as

$$\dot{\mathbf{p}}^{\mathcal{H}}(t) = \mathbf{A}\dot{\mathbf{p}}(t) = \mathbf{A}\kappa(\mathbf{A} - \mathbf{I}_{2N})\mathbf{p}(t) = \kappa(\mathbf{A}^2 - \mathbf{A})\mathbf{p}(t) = \mathbf{0}. \tag{24}$$

Notice $\dot{\mathbf{p}}(t) = -\kappa\mathbf{e}(t)$ from (21). As $\mathbf{p}^{\mathcal{H}}(t)$ stays constant, $\dot{\mathbf{e}}(t) = \dot{\mathbf{p}}(t)$ and thus $\dot{\mathbf{e}}(t) = -\kappa\mathbf{e}(t)$, concluding the proof. ■

To study the stability for double-integrator dynamics, we assume the system is at rest initially, i.e., $\dot{\mathbf{p}}(t = 0) = \mathbf{0}$.

Theorem 2: Under the double-integrator control law (22), $\mathbf{p}^{\mathcal{H}}(t)$ is invariant and the control error $\mathbf{e}(t)$ converges to zero globally and exponentially fast. Moreover, if $\kappa_2 \geq 2\sqrt{\kappa_1} > 0$, the convergence to zero of every one of the $2N$ components of $\mathbf{e}(t)$ is monotonic.

Proof: For double-integrator dynamics, $\ddot{\mathbf{p}}(t) = \mathbf{u}(t)$. Under (22), we have

$$\begin{aligned}\ddot{\mathbf{p}}^{\mathcal{H}}(t) &= \mathbf{A}\ddot{\mathbf{p}}(t) = \mathbf{A}\big(\kappa_1(\mathbf{A} - \mathbf{I}_{2N})\mathbf{p}(t) + \kappa_2(\mathbf{A} - \mathbf{I}_{2N})\dot{\mathbf{p}}(t)\big) \\ &= \kappa_1(\mathbf{A}^2 - \mathbf{A})\mathbf{p}(t) + \kappa_2(\mathbf{A}^2 - \mathbf{A})\dot{\mathbf{p}}(t) = \mathbf{0}.\end{aligned} \tag{25}$$

Therefore, since by assumption $\dot{\mathbf{p}}^{\mathcal{H}}(t = 0) = \mathbf{0}$, $\mathbf{p}^{\mathcal{H}}$ is invariant, i.e., $\dot{\mathbf{p}}^{\mathcal{H}}(t) = \mathbf{0}$ $\forall t$, and $\mathbf{p}^{\mathcal{H}}(t) = \mathbf{p}^{\mathcal{H}}(t = 0)$ $\forall t$. Notice $\ddot{\mathbf{p}}(t) = -\kappa_1\mathbf{e}(t) - \kappa_2\dot{\mathbf{e}}(t)$ from (22). As $\mathbf{p}^{\mathcal{H}}(t)$ is constant, we have that $\ddot{\mathbf{e}}(t) = \ddot{\mathbf{p}}(t)$. Hence,

$$\ddot{\mathbf{e}}(t) = -\kappa_1\mathbf{e}(t) - \kappa_2\dot{\mathbf{e}}(t). \tag{26}$$

Let us denote by $e_i(t) \in \mathbb{R}$ the i-th component of the $2N \times 1$ vector $\mathbf{e}(t)$. The dynamics of every $e_i(t)$ are uncoupled from the dynamics of the other components and they have the form $\ddot{e}_i(t) = -\kappa_1 e_i(t) - \kappa_2\dot{e}_i(t)$. This can be expressed as the system $[\dot{e}_i(t), \ddot{e}_i(t)]^{\intercal} = \mathbf{C} \cdot [e_i(t), \dot{e}_i(t)]^{\intercal}$ with $\mathbf{C} = [[0, -\kappa_1]^{\intercal}, [1, -\kappa_2]^{\intercal}]$. The characteristic equation of $\mathbf{C}$ is $\lambda^2 + \kappa_2\lambda + \kappa_1 = 0$. As κ_1 and κ_2 are positive, the eigenvalues, λ, of $\mathbf{C}$ have negative real parts. Hence, the system is stable and $e_i(t)$ converges to zero globally and exponentially fast. Moreover, if $\kappa_2 \geq 2\sqrt{\kappa_1}$, λ are real; hence, $e_i(t)$ converges to zero monotonically without overshooting. ■

C. Dynamics of centroid and scale

The centroid and the scale are important variables to consider for characterizing the state of the team. We define the centroid $\mathbf{g}_{\mathbf{p}} \in \mathbb{R}^2$ and scale $s_{\mathbf{p}} \in \mathbb{R}_{\geq 0}$ as

$$\mathbf{g}_{\mathbf{p}} = \frac{1}{N}\sum_{n\in\mathcal{N}} \mathbf{p}_n = \frac{1}{N}(\mathbf{1}_N \otimes \mathbf{I}_2)^{\intercal}\mathbf{p}, \tag{27}$$

$$s_{\mathbf{p}} = \frac{1}{N}\sum_{n\in\mathcal{N}} ||\mathbf{p}_n - \mathbf{g}_{\mathbf{p}}||^2 = \frac{1}{N}||\mathbf{p} - \mathbf{1}_N \otimes \mathbf{g}_{\mathbf{p}}||^2. \tag{28}$$

Note that $s_{\mathbf{p}}$ characterizes the size of the team relative to the centroid. We study the dynamics of these variables next.

Proposition 1: If it holds that for every agent n, $\dot{\mathbf{p}}_n(t) = -\mu\nabla_{\mathbf{p}_n}\gamma$ with $\mu > 0 \in \mathbb{R}$, then (i) the centroid $\mathbf{g}_{\mathbf{p}}(t)$ is invariant and (ii) the scale $s_{\mathbf{p}}(t)$ is nonincreasing over time.

Proof: As a first step in the study of the centroid's dynamics, consider a configuration $\mathbf{p} = [\mathbf{q}^{\intercal}, ..., \mathbf{q}^{\intercal}]^{\intercal} = \mathbf{1}_N \otimes \mathbf{q}$ for some $\mathbf{q} \in \mathbb{R}^2$. The DFT of the sequence corresponding to this configuration for $k = 0, 1, ..., N-1$ is

$$\mathbf{d}_k = \sum_{n\in\mathcal{N}} \mathbf{R}_{kn}\mathbf{p}_n = (\sum_{n\in\mathcal{N}} \mathbf{R}_{kn})\mathbf{q}. \tag{29}$$

Clearly, $\mathbf{d}_0 = N\mathbf{q}$. For every k different from zero, it holds that $\sum_{n\in\mathcal{N}} \mathbf{R}_{kn} = \mathbf{0}$, because the angles of these summed rotations are equispaced samples covering the range from 0 to 2π. Hence, $\mathbf{d}_k = \mathbf{0}$ $\forall k \neq 0$. Therefore, the configuration does not change after truncating the DFT; i.e., $\mathbf{d}^{\mathcal{H}} = \mathbf{d}$, and hence $\mathbf{p}^{\mathcal{H}} = \mathbf{p}$. From (20), this implies the gradient is zero and $(\mathbf{A} - \mathbf{I}_{2N})(\mathbf{1}_N \otimes \mathbf{q}) = \mathbf{0}$ for any $\mathbf{q} \in \mathbb{R}^2$. Then, $(\mathbf{A} - \mathbf{I}_{2N})(\mathbf{1}_N \otimes \mathbf{I}_2) = \mathbf{0}$ too. Now, we compute the centroid dynamics under the assumed motion for an arbitrary $\mathbf{p}$ as

$$\dot{\mathbf{g}}_{\mathbf{p}} = \frac{1}{N}(\mathbf{1}_N \otimes \mathbf{I}_2)^{\intercal}\dot{\mathbf{p}} = \frac{\mu}{N}(\mathbf{1}_N \otimes \mathbf{I}_2)^{\intercal}(\mathbf{A} - \mathbf{I}_{2N})\mathbf{p}. \tag{30}$$

As $(\mathbf{1}_N \otimes \mathbf{I}_2)^{\intercal}(\mathbf{A} - \mathbf{I}_{2N})$ in this equation is equal to $\big((\mathbf{A} - \mathbf{I}_{2N})(\mathbf{1}_N \otimes \mathbf{I}_2)\big)^{\intercal}$, we conclude that $\dot{\mathbf{g}}_{\mathbf{p}} = \mathbf{0}$ using the above.

This article has been accepted for publication in IEEE Control Systems Letters. This is the author's version which has not been fully edited and content may change prior to final publication. Citation information: DOI 10.1109/LCSYS.2023.3331245

Next, we analyze the dynamics of the scale. We have

$$\dot{s}_{\mathbf{p}} = \frac{2}{N}(\mathbf{p} - \mathbf{1}_N \otimes \mathbf{g}_{\mathbf{p}})^{\intercal}(\dot{\mathbf{p}} - \mathbf{1}_N \otimes \dot{\mathbf{g}}_{\mathbf{p}}) = \frac{-4\mu\gamma}{N} \leq 0, \quad (31)$$

where we used $\dot{\mathbf{g}}_{\mathbf{p}} = \mathbf{0}$, $\dot{\mathbf{p}} = \mu(\mathbf{A} - \mathbf{I}_{2N})\mathbf{p}$, and then $(\mathbf{1}_N \otimes \mathbf{g}_{\mathbf{p}})^{\intercal}(\mathbf{A} - \mathbf{I}_{2N}) = \big((\mathbf{A} - \mathbf{I}_{2N})(\mathbf{1}_N \otimes \mathbf{g}_{\mathbf{p}})\big)^{\intercal} = \mathbf{0}$. ■

Remark 1: Preserving the centroid is advantageous from the standpoint of motion efficiency, as the agents reach the desired formation without requiring a superfluous translation of the team as a whole. As $s_{\mathbf{p}}$ is nonincreasing, its minimum value over time occurs at the final configuration, $\mathbf{p}(t \to \infty) = \mathbf{p}^{\mathcal{H}}(t = 0)$, which is an invariant configuration represented by the low-frequency Fourier descriptors of $\mathtt{P}(t = 0)$. Two relevant properties are, then, that (i) $s_{\mathbf{p}}(t \to \infty)$ depends on the initial configuration, and (ii) while theoretically $s_{\mathbf{p}}(t \to \infty)$ can be zero in isolated degenerate cases where the content of $\mathtt{P}(t = 0)$ at the relevant low frequencies is exactly zero, $s_{\mathbf{p}}$ is greater than zero in general. In practice, task constraints (e.g., interagent safety distances) automatically bound the value of the scale $s_{\mathbf{p}}$ from below and allowing this value to vary makes the behavior more adaptable; still, the ability to control the scale is also important and could be added by using, e.g., further control terms or leader agents.

D. Robustness to perturbed motions

The fact that our control approach is gradient-based endows it with robustness to a certain type of motion perturbations. Specifically, if an agent's actual motion vector is equal to the ideal vector (i.e., the negative gradient of γ) up to a positive scaling and a rotation of less than $\pi/2$ in absolute value, the team will still converge to the desired formation. This is important as in practice, agent motions are subject to various perturbations, e.g., measurement error and actuation disturbance. This robustness property was studied in, e.g., [18, Sec. III.C]. We study it for our system next.

Proposition 2: Assume that for every agent n, $\dot{\mathbf{p}}_n = -w_n \mathbf{G}_n \nabla_{\mathbf{p}_n}\gamma$ where $w_n > 0 \in \mathbb{R}$ and $\mathbf{G}_n = [[\cos(\alpha_n), \sin(\alpha_n)]^{\intercal}, [-\sin(\alpha_n), \cos(\alpha_n)]^{\intercal}]$ with $|\alpha_n| < \pi/2$. Furthermore, assume $\mathbf{g}_{\mathbf{p}}(t)$ and $s_{\mathbf{p}}(t)$ remain bounded $\forall t$. Then, the team converges to the desired formation.

Proof: As the centroid $\mathbf{g}_{\mathbf{p}}(t)$ and scale $s_{\mathbf{p}}(t)$ remain bounded, there exists a compact set $\Omega = \{\mathbf{p} : ||\mathbf{p}|| \leq r\}$ for some finite $r > ||\mathbf{p}(t = 0)||$ such that $\mathbf{p}(t = 0) \in \Omega$ and Ω is positively invariant. Now, consider the continuously differentiable function $\gamma(\mathbf{p})$. We have

$$\dot{\gamma} = \sum_{n \in \mathcal{N}} (\nabla_{\mathbf{p}_n}\gamma)^{\intercal} \cdot \dot{\mathbf{p}}_n = -\sum_{n \in \mathcal{N}} (\nabla_{\mathbf{p}_n}\gamma)^{\intercal} \cdot w_n \mathbf{G}_n \nabla_{\mathbf{p}_n}\gamma$$
$$= -\sum_{n \in \mathcal{N}} w_n \cos(\alpha_n) ||\nabla_{\mathbf{p}_n}\gamma||^2. \quad (32)$$

Note $w_n \cos(\alpha_n) > 0 \ \forall n \in \mathcal{N}$. Therefore, $\dot{\gamma} \leq 0 \ \forall t$. Then, by virtue of LaSalle's invariance theorem [19, Thm. 4.4], $\mathbf{p}$ converges to the largest invariant set in Ω where $\dot{\gamma} = 0$. From (32), the condition $\dot{\gamma} = 0$ implies $\nabla_{\mathbf{p}_n}\gamma = \mathbf{0} \ \forall n \in \mathcal{N}$, i.e., $\nabla_{\mathbf{p}}\gamma = \mathbf{0}$. From (20), this implies $\mathbf{p}(t) = \mathbf{p}^{\mathcal{H}}(t)$. ■

Remark 2: From Prop. 2, our control laws (21), (22), which are based on following the negative gradient of γ, are robust to perturbations of the considered type. From Prop. 1, when following the negative gradient of γ, the centroid $\mathbf{g}_{\mathbf{p}}(t)$ is invariant and the scale $s_{\mathbf{p}}(t)$ is nonincreasing. Therefore, it is reasonable to assume, as we did in Prop. 2, that the centroid and the scale remain bounded under the perturbations.

E. Implementation of the controller

Next, we explain how every agent $n \in \mathcal{N}$ can implement the proposed controller. Let $\mathbf{A}_n \in \mathbb{R}^{2 \times 2N}$ denote the matrix formed by the rows of $\mathbf{A}$ with indices $2n + 1$ and $2n + 2$. Then, for the single-integrator case, from (21), we have

$$\mathbf{u}_n(t) = \kappa(\mathbf{A}_n \mathbf{p}(t) - \mathbf{p}_n(t)). \quad (33)$$

In the double-integrator case, from (22), we have

$$\mathbf{u}_n(t) = \kappa_1(\mathbf{A}_n \mathbf{p}(t) - \mathbf{p}_n(t)) + \kappa_2(\mathbf{A}_n \dot{\mathbf{p}}(t) - \dot{\mathbf{p}}_n(t)). \quad (34)$$

The control computation for every agent n requires the knowledge of the positions (and, in the double-integrator case, also the velocities) of all agents. A possible implementation option is to use a central node. An alternative is a setup where every agent computes its control law independently. As our approach assumes the knowledge of the current states of all agents, it has limited scalability and robustness to failure, which makes its applicability difficult in the case of, e.g., large swarms. A distributed implementation based on communications could improve on these fronts [20], [21]. Note that the agents can use relative position measurements, i.e., a specific absolute coordinate origin is not needed. To see this, assume an agent uses a coordinate origin $\mathbf{p}_r \in \mathbb{R}^2$, i.e., it implements the controller using measurements $\mathbf{p} - \mathbf{1}_N \otimes \mathbf{p}_r$. As $(\mathbf{A} - \mathbf{I}_{2N})(\mathbf{1}_N \otimes \mathbf{p}_r) = \mathbf{0}$ for any $\mathbf{p}_r$, clearly the controller is independent of $\mathbf{p}_r$. The agent's motion does not change either if the controller is computed in a rotated reference frame. This is because $(\mathbf{A} - \mathbf{I}_{2N})\mathbf{p}$ applies scalar weights to the positions in $\mathbf{p}$. Following, e.g., [2, Sec. V-A.1], this makes our controller invariant to rotation of the reference frame. These arguments also apply to the velocity measurements.

Our controller does not avoid collisions between agents. One practical way to incorporate collision avoidance (albeit without full guarantee of formation achievement) is via control barrier functions [22], as shown in example 4 in Sec. IV.

IV. Simulation Examples

We report on four examples run in MATLAB, with results presented in Fig. 1. In example 1 we use $N = 8$, $H = 3$, and the agents are single integrators, with control gain $\kappa = 1$. The results agree with our theoretical analysis and the team converges to a discretized ellipse. Example 2 has the same parameters and the same initial configuration, but we introduce perturbations to the magnitude and direction of every $\mathbf{u}_n = \dot{\mathbf{p}}_n$ as in Prop. 2. As expected, the team still converges to the desired formation, but the achieved ellipse is different with respect to example 1. In example 3 we use $N = 15$, $H = 5$, and double-integrator agents with control gains $\kappa_1 = 1$, $\kappa_2 = 3$. Again we obtain the expected behavior. The shape of the desired formation is more complex than an ellipse because we used more Fourier descriptors. Finally, our example 4 is run on the Robotarium simulator [23] with $N = 12$ unicycle

This article has been accepted for publication in IEEE Control Systems Letters. This is the author's version which has not been fully edited and content may change prior to final publication. Citation information: DOI 10.1109/LCSYS.2023.3331245

agents and $H = 5$. We use control (21) with $\kappa = 2$ and built-in dynamic model conversion and collision avoidance routines. Three external agents move toward the team, stopping at $t = 20$ s. From an initial circular configuration with radius 70 cm, the formation agents react by avoiding collision while continuously moving toward keeping the desired formation, eventually converging to it. As the team is not constrained to form a prescribed pattern (e.g., an ellipse), it is able to adapt its shape more flexibly, while remaining on a low-frequency closed curve. This behavior is interesting in enclosing tasks.

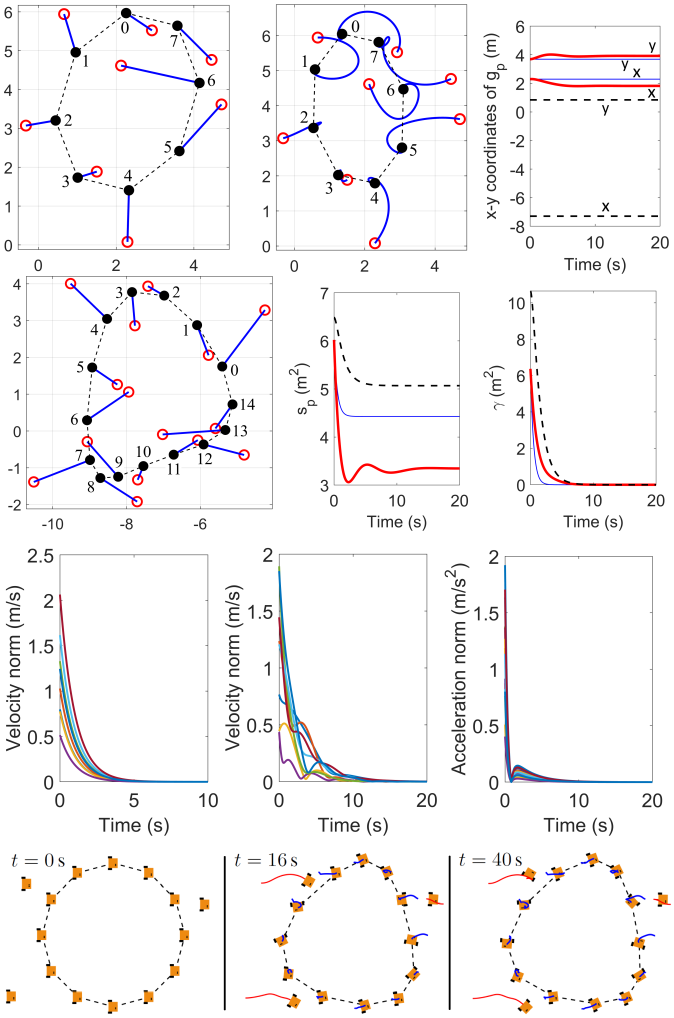

Fig. 1. Simulation results for examples (ex.) 1 through 4. In each row (i), from left to right: (1) Paths for ex. 1 and ex. 2, centroid evolution for ex. 1-3. (2) Paths for ex. 3, scale and cost evolutions for ex. 1-3. Path plots show: agent paths (blue solid lines), initial positions (red hollow circles), final positions (black solid circles) with agent indices and joined by dashed lines. The units of the axes are meters. In the time evolution plots, blue thin solid lines are for ex. 1, red thick solid lines for ex. 2, black dashed lines for ex. 3. (3) Agents' control input norms for ex. 1-3. (4) Snapshots from ex. 4. Agent configurations and paths are shown. Formation agents are joined by dashed lines. The values of $\gamma(t)$ in m^2 are $\gamma = \mathbf{0}$ at $\mathbf{0}$ s, $\gamma = \mathbf{1.6 \cdot 10^{-3}}$ at $\mathbf{16}$ s, $\gamma = \mathbf{2.6 \cdot 10^{-6}}$ at $\mathbf{40}$ s.

V. Conclusion

We have presented a novel approach for specifying and controlling planar multiagent formations exploiting Fourier descriptors to deploy agents along a low-frequency discretized closed curve. Future work directions include: (i) developing a distributed version of the proposed approach, to increase its scalability and robustness, and (ii) extending the approach to address higher-level tasks requiring the team to adapt its shape, centroid and scale dynamically.

References

[1] K.-K. Oh, M.-C. Park, and H.-S. Ahn, "A survey of multi-agent formation control," *Automatica*, vol. 53, pp. 424–440, 2015.

[2] S. Zhao, "Affine formation maneuver control of multiagent systems," *IEEE Trans. Automat. Contr.*, vol. 63, no. 12, pp. 4140–4155, 2018.

[3] M. Aranda, J. A. Corrales, and Y. Mezouar, "Deformation-based shape control with a multirobot system," in *Proc. IEEE Int. Conf. Robot. Automat.*, 2019, pp. 2174–2180.

[4] F. Mehdifar, F. Hashemzadeh, M. Baradarannia, and M. de Queiroz, "Finite-time rigidity-based formation maneuvering of multiagent systems using distributed finite-time velocity estimators," *IEEE Trans. Cybern.*, vol. 49, no. 12, pp. 4473–4484, 2019.

[5] S. Zhao and D. Zelazo, "Bearing rigidity and almost global bearing-only formation stabilization," *IEEE Trans. Automat. Contr.*, vol. 61, no. 5, pp. 1255–1268, 2016.

[6] N. Michael and V. Kumar, "Controlling shapes of ensembles of robots of finite size with nonholonomic constraints," in *Robot.: Sci. Syst. IV*. The MIT Press, 2009, pp. 41–48.

[7] C. J. Stamouli, C. P. Bechlioulis, and K. J. Kyriakopoulos, "Multi-agent formation control based on distributed estimation with prescribed performance," *IEEE Robot. Automat. Lett.*, vol. 5, no. 2, pp. 2929–2934, 2020.

[8] G. Fedele, L. D'Alfonso, and A. Bono, "A discrete-time model for swarm formation with coordinates coupling matrix," *IEEE Control Syst. Lett.*, vol. 4, no. 4, pp. 1012–1017, 2020.

[9] G. C. Maffettone, A. Boldini, M. Di Bernardo, and M. Porfiri, "Continuification control of large-scale multiagent systems in a ring," *IEEE Control Syst. Lett.*, vol. 7, pp. 841–846, 2023.

[10] J. G. Proakis and D. G. Manolakis, *Digital signal processing (3rd ed.): Principles, algorithms, and applications*. Prentice-Hall, Inc., 1996.

[11] R. C. González and R. E. Woods, *Digital image processing, 3rd Edition*. Pearson Education, 2008.

[12] Y. Zhao and S. Belkasim, "Multiresolution Fourier descriptors for multiresolution shape analysis," *IEEE Signal Process. Lett.*, vol. 19, no. 10, pp. 692–695, 2012.

[13] D. Navarro-Alarcon and Y.-H. Liu, "Fourier-based shape servoing: A new feedback method to actively deform soft objects into desired 2-D image contours," *IEEE Trans. Robot.*, vol. 34, no. 1, pp. 272–279, 2018.

[14] S. Evren and M. Unel, "Planar formation control of swarm robots using dynamical elliptic Fourier descriptors," *Trans. Inst. Meas. Control*, vol. 37, no. 5, pp. 661–671, 2015.

[15] B. Zhang et al., "Fourier-based multi-agent formation control to track evolving closed boundaries," *IEEE Trans. Circuits Syst. I: Regul. Pap.*, vol. 70, no. 11, pp. 4549–4559, 2023.

[16] L. Briñón-Arranz, A. Seuret, and A. Pascoal, "Circular formation control for cooperative target tracking with limited information," *J. Frank. Inst.*, vol. 356, no. 4, pp. 1771–1788, 2019.

[17] G. López-Nicolás, M. Aranda, and Y. Mezouar, "Adaptive multirobot formation planning to enclose and track a target with motion and visibility constraints," *IEEE Trans. Robot.*, vol. 36, no. 1, pp. 142–156, 2020.

[18] K. Fathian, S. Safaoui, T. H. Summers, and N. R. Gans, "Robust distributed planar formation control for higher order holonomic and nonholonomic agents," *IEEE Trans. Robot.*, vol. 37, no. 1, pp. 185–205, 2021.

[19] H. K. Khalil, *Nonlinear systems; 3rd ed.* Prentice-Hall, 2002.

[20] G. Antonelli, F. Arrichiello, F. Caccavale, and A. Marino, "Decentralized time-varying formation control for multi-robot systems," *Int. J. Robot. Res.*, vol. 33, no. 7, pp. 1029–1043, 2014.

[21] M. Aranda, G. López-Nicolás, C. Sagüés, and M. M. Zavlanos, "Coordinate-free formation stabilization based on relative position measurements," *Automatica*, vol. 57, pp. 11–20, 2015.

[22] L. Wang, A. D. Ames, and M. Egerstedt, "Safety barrier certificates for collisions-free multirobot systems," *IEEE Trans. Robot.*, vol. 33, no. 3, pp. 661–674, 2017.

[23] S. Wilson et al., "The Robotarium: Globally impactful opportunities, challenges, and lessons learned in remote-access, distributed control of multirobot systems," *IEEE Control Syst. Mag.*, vol. 40, no. 1, pp. 26–44, 2020.